Sensors and Actuators A 240 (2016) 57–69

Contents lists available at ScienceDirect

Sensors and Actuators A: Physical

journal homepage: www.elsevier.com/locate/sna

Calibration and performance assessment of an innovative high-temperature cavitometer

I. Tzanakis[a,f,*], M. Hodnett[b], G.S.B. Lebon[c], N. Dezhkunov[d], D.G. Eskin[a,e]

[a] Brunel Centre for Advanced Solidification Technology (BCAST), Brunel University, Uxbridge, Middlesex UB8 3PH, UK
[b] Acoustics and Ionising Radiation Division, National Physical Laboratory, Hampton Road, Teddington, Middlesex TW11 0LW, UK
[c] Centre for Numerical Modelling and Process Analysis, University of Greenwich, London SE10 9LS, UK
[d] Belarusian State University of Informatics and Radioelectronics, Minsk 220013, Belarus
[e] Tomsk State University, Tomsk 634050 Russia
[f] Faculty of Technology, Design and Environment, Oxford Brookes University, Wheatley Campus, Wheatley OX33 1HX, UK

ARTICLE INFO

Article history:
Received 27 August 2015
Received in revised form
21 December 2015
Accepted 13 January 2016
Available online 15 January 2016

Keywords:
Cavitation
Cavitometer
Liquid metal
Sensor
Acoustic emissions
Frequency spectrum
Sonochemistry

ABSTRACT

This paper describes a series of systematic experimental studies to evaluate the performance of a high-temperature cavitometer under well-controlled conditions. The cavitometer was specifically designed for measurements in liquid metals: it operates through a long tungsten waveguide (probe), providing thermal protection to the piezo sensing elements placed outside the hot area, and with sufficient bandwidth to enable the monitoring of broadband acoustic emissions associated with cavitation activity. It was calibrated electrically, and acoustically, at kHz and MHz frequencies, and so can be used to estimate acoustic pressures (in Pa), providing physical, and consequently practical, meaning to cavitation measurements within liquid metals. Results obtained from ultrasonic sources in a cylindrical vessel using water showed that the cavitometer is a reliable and robust device for characterizing direct field acoustic pressures and broadband emissions from the resulting cavitation. Additionally, preliminary characterization of the real-time acoustic pressures during ultrasonic processing of liquid aluminium (Al) in a standard clay-graphite crucible were performed for the first time. The use of the calibrated cavitometer will establish a more generalized approach for measuring the actual acoustic pressures over a broad range of liquid temperatures within a sonicated medium, demonstrating its potential use as a tool for optimizing, controlling, and scaling-up processes.

1. Introduction

Acoustic cavitation is the formation of highly energetic gas or vapour bubbles, primarily from pre-existing nuclei, within a sonicated liquid volume due to local pressure fluctuations of the acoustic field. Bubbles grow during the rarefaction phase and then collapse during the compression phase. Cavitation is usually distinguished into two classes of behaviour: non-inertial (or stable) cavitation, and inertial (or transient) cavitation. Two categories of stable bubbles may be distinguished: (a) pulsating linearly (low energy bubbles) contributing to an increase in the fundamental frequency component peak f_0 and its harmonics i.e. nf_0; (where n is an integer) and (b) pulsating and collapsing nonlinearly (higher energy bubbles) in the so-called "repetitive transient cavitation" regime, generating sub- and ultra-harmonic peaks i.e. nf_0, $nf_0/2$, $nf_0/4$ as well as distinctive broadband signals [1]. Transient cavitation is associated with the dynamics of the collapse and is characterised by material erosion [2], sonocapillary effect [3], biomedicine [4] etc. and the generation of sub- and ultra-harmonic peaks as well as an increase in the broadband signal, the so-called cavitation noise, in the acoustic spectrum. Cavitation noise has long been considered as a phenomenon that contains information about the cavitation zone [5–9] and for this reason, it is a versatile candidate for cavitation activity monitoring.

Many commercially available acoustic cavitation devices operate in the range 20–50 kHz; yet acoustic emissions from collapsing bubble clouds extend readily to MHz frequencies, such is the non-linear nature of energy redistribution. This enables detailed information to be captured and extracted when suitable detectors are applied. Since the pioneering work of Esche [10] in the 1950s, the detection of acoustic emissions from cavitating bubbles or a bubbly cloud has been extensively studied, with the majority of these studies performed in aqueous media. The frequency spectra of acoustic cavitation noise have been studied by many groups

* Corresponding author.
E-mail address: iakovos.tzanakis@brunel.ac.uk (I. Tzanakis).

http://dx.doi.org/10.1016/j.sna.2016.01.024

[7–9,11]. The broadband cavitation noise spectrum has the form of line components overlaid on a wide band (continuous) noise spectrum. The presence of line spectra and their harmonics is usually related to the nonlinear pulsation of cavitation bubbles [6] or the nonlinear propagation of ultrasound in bubbly liquid [12]. The presence of the wide band component in a cavitation noise spectrum is generally attributed to the generation of shock waves. A shock wave can be represented mathematically by a Dirac delta-function, and the frequency spectrum of the delta-function is white noise [13]. It has been shown [11] that the appearance of sonoluminescence emissions from the cavitating regions of a fluid correlates with the appearance of broadband acoustic emissions, showing that both phenomena relate to bubble collapse [14,15]. Thus, the higher the number of collapsing bubbles in the cavitating fluid, and the greater the energy or 'violence' with which they collapse, the higher the integrated value of the broadband acoustic emission. However, obtaining a real-time indication of cavitation activity based on acoustic detection of emissions is complex because shielding and scattering effects can potentially reduce the emitted acoustic pressure levels travelling through the liquid media, even over length scales of millimetres [16], and defining the spatial resolution of any sensor can also be difficult.

Stable cavitation may be relevant in some applications of high power ultrasound such as degassing [17–19], while transient cavitation is associated with technologically important phenomena such as grain refinement in solidification of metals and deagglomeration of reinforcing particles in composite materials [20,21], as well as cleaning and sonochemistry [22]. In liquid metals, the effective action of high pressure acoustic waves is attributed to the occurrence of mechanically violent cavitation bubbles, a mechanism that is still under scrutiny due to the experimental challenges involved [21–25]. In recent years, there has been an increased interest in fundamental and applied investigations of metal solidification promoted by ultrasound since ultrasonic treatment improves the material properties and structure of the solidified metal [21]. However, temperature requirements, medium opacity, and lack of advanced equipment for measuring cavitation activity have restricted investigations of cavitation bubble dynamics within liquid metals. These difficulties have impeded the industrial take-up of ultrasonic vibrations in liquid-metal processing. Thus, despite the well-known and growing technological importance of high power ultrasound, no standardised measurement methods applicable to measuring the cavitation activity and map acoustic pressures in the melt exist to date and very few studies have been conducted to characterize cavitation activity in liquid metals [21,26,27].

In a recent study, a cavitometer similar to the one used in this study was used by Komarov et al. [26] to characterize cavitation intensities in a molten aluminium (Al) alloy. The filter settings of the cavitometer that they used for measuring cavitation noise include six different frequency bands. In their results, the cavitation activity within the liquid Al alloy is presented in terms of the electrical output of the cavitometer sensor (mV). However, these results cannot be practically applied, for example, in the validation of numerical acoustic models, as the output provided by the cavitometer is not in useful physical units, i.e. Pa. Thus, in the current study, calibration of the high-temperature cavitometer was performed at the National Physical Laboratory (NPL), UK. Although carried out under well-controlled conditions in the absence of cavitation, the derived calibration sensitivity factors can be used to estimate acoustic pressures (in Pa) in the presence of cavitation, providing physical and, consequently practical, meaning to cavitation measurements within liquid metals. After the calibration process, a comparison with a cavitation sensor (Cavisensor) developed at NPL [28,29] was performed under aqueous conditions. Preliminary measurements with the high-temperature cavitometer were then conducted in liquid Al.

2. Description of cavitometer

The cavitometer (Fig. 1) was developed and manufactured by the Belarusian State University of Informatics and Radioelectronics, Belarus, and is specifically designed to measure cavitation activity in high-temperature and high-power ultrasonic fields, i.e. in molten metals. The cavitometer consists of an electronic block device (ICA-3HT) and a hydrophone designed to be protected against heat and cavitation erosion. The hydrophone has a probe (receiver) that is attached to a piezoceramic plate. The receiver acts as a waveguide, coupling the acoustic signal from the cavitation zone to the piezoceramic plate. The waveguide is long so that the distance between the hot metal and the sensitive piezoelectric element as well as the casing of the latter ensures the protection from heat both by conduction and radiation. The hydrophone is electrically connected to the electronic block that displays and processes the electrical signal produced by the piezoelectric probe in response to acoustical stimulation. Various settings and outputs are available for optimising the detection regime and for enabling offline signal monitoring and analysis using external oscilloscopes and voltmeters.

It is impossible to use conventional hydrophones (mechanical or piezoelectric) for direct measurements at temperatures higher than 150 °C due to thermal stability of a piezoceramic membrane or a plate. The cavitometer hydrophone receiver is hence made of a tungsten alloy (97.3–97.8% W), such as that used in welding electrodes. Tungsten has a much higher melting temperature than aluminium (3420 °C vs 660 °C), very low solubility in liquid aluminium, and high thermal stability of properties [30]. The manufacturer of the cavitometer has estimated theoretically the temperature variation of the piezoceramic plate with time for different immersed lengths of the tungsten probe in a molten alloy at temperatures near to 800 °C. On the basis of these estimates, the dimensions of the tungsten waveguide were chosen to be 500 mm in length and 4 mm in diameter, which allows for 10–15 min of continuous measurements in liquid Al, after which the cavitometer might overheat. The disadvantage of a tungsten alloy is its high ultrasound absorption coefficient. This leads to signal losses in the waveguide, especially for frequency components approaching MHz ranges.

The working principle of the cavitometer is based on the detection of acoustic signals generated in a fluid, from both the direct field and acoustic emissions produced by cavitation. A raw broadband signal is received from the cavitometer and can be analysed and displayed on the accompanying electronics, or accessed via BNC connection and processed offline by appropriate instrumentation and software. Processing offline allows measured voltages to be converted to acoustic pressure using the calibration described in the following sections. Measurement of the cavitation noise carried out using the cavitometer positioned within or close to the cavitation zone in a fluid is used to provide a measurement of the acoustic emissions generated by the cavitation bubbles. Specifically, the integrated cavitation noise over the frequency spectrum up to 10 MHz is considered as an indicator of total cavitation activity. It has been shown in experiments similar to [11] that, for ultrasonic fields having driving frequencies in the range 20–25 kHz, transient cavitation is accompanied by the appearance of frequencies higher than $10f_0$. Based on this, we assume that the integral intensity of the cavitometer hydrophone output in the range of frequencies $10f_0$ −10 MHz represents transient cavitation activity, with the onset of inertial cavitation indicated by the first peak of the generated sub-harmonic [31]. Total cavitation activity, includ-

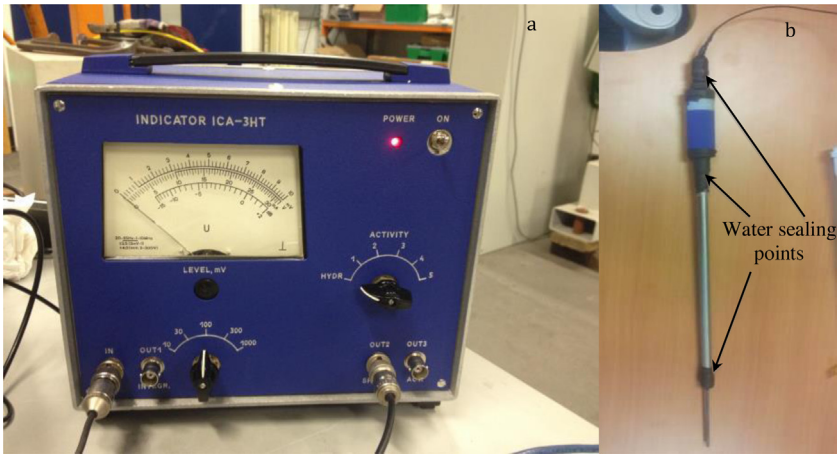

Fig. 1. A cavitometer device (a) ICA-3HT electronic unit and (b) a high-temperature hydrophone connected to the unit (the hydrophone is sealed for calibration in water).

ing stable linear cavitation, is given by the integration of the output signal in the whole range of the acoustic spectrum.

Various signal processing options are provided by the ICA-3HT electronics unit, and these are described and tested briefly in Section 3: their purpose is to provide a range of system bandwidths, which can then enable the user to infer information on the relative 'violence' of cavitation activity in a given sonicated fluid. For the majority of studies presented in this paper, the unprocessed cavitometer probe signal was used, with separate oscilloscopes and meters.

3. Calibration process

The electrical and acoustical characteristics of the cavitometer were investigated using calibrated devices, methods, and facilities developed at NPL. Results were analysed to investigate signal relationships, and to consider the uncertainties in subsequent acoustical measurements.

3.1. Electrical characterisation

Prior to undertaking any acoustical measurements, the operation of the cavitometer electronics was investigated using stable, controllable electrical signals. Parameters such as frequency response, linearity, and loading effect were extensively tested.

A Keithley 3390 signal generator was used to make measurements of the frequency response of the six 'Activity' settings of the ICA-3HT cavitometer unit. The value displayed on the needle scale was monitored for an applied signal level of 100 mV p–p, with the cavitometer sensitivity set to 100, whilst the Keithley signal was frequency swept. The signal filtering with the corresponding switches of ICA-3HT unit is shown in Table 1. The cavitometer electronics is hence capable of detecting signals up to 9.5 MHz, which, if replicated in acoustic tests, would correlate with inertial cavitation emissions.

The values displayed on the needle scale of the ICA-3HT unit were compared with those measured by external meters connected to OUT 1. For this, a Rohde and Schwarz (Munich, Germany) URE-3 RMS/Peak meter was used to test the input signal, and then monitor the output signal. This was carried out for a 1 V peak-to-peak input signal, at frequencies of 20 kHz and 1 MHz, for the three least sensitive scales of the needle display. Results are shown in Fig. 2a and b. In both of these figures, the secondary *Y*-axis shows the signal measured by the URE-3 and the primary *Y*-axis show the needle readings. The needle meter readings agree well with the applied signal level, across all sensitivity ranges, showing a linearity response, but there is a systematic loading effect on OUT 1, of approximately 30% at 20 kHz, and 20% at 1 MHz, even though the URE-3 input was correctly terminated. This loading effect is accounted for in acoustic pressure estimates when OUT 1 is used.

Similar tests were carried out to examine the frequency response of the most likely used measurement channels (3 and 4) for detecting inertial cavitation emissions, by holding the Keithley drive level constant (100 mV p–p), and again sweeping the frequency of the sinusoid. For this, OUT 2 (filtered signal output) was connected to an Agilent 3024A oscilloscope (Santa Clara, CA, USA). The cavitometer was tested in its '100' sensitivity range setting. As before, the cavitometer output voltage was monitored using the URE-3. Results are shown in Fig. 3.

For both filter channel positions, there is good shape agreement between the displayed (needle) value and the OUT 2 signal, albeit with a considerable difference in levels: this shows the amplification effect applied internally by the unit.

3.2. Acoustical characterisation

3.2.1. Probe calibration

For these tests, the cavitometer hydrophone was fully immersed in a large test tank. Points of likely water ingress were protected using self-amalgamating tape, and silicone rubber solution as

Table 1
Frequency response of the six 'activity' settings available in the cavitometer unit.

Activity setting	Specified threshold (kHz)	First detection of signal (kHz)	Upper limit (kHz)[a]	Stable level range (kHz)
HYDR	N/A	0.25	380	12–380
1	N/A	90	600	450–600
2	N/A	170	1150	850–1150
3	350	220	1200	Not measured
4	650	430	2500	Not measured
5	3700	2700	9500	Not measured

[a] Defined as the value at which the needle meter level starts to decrease following a plateau.

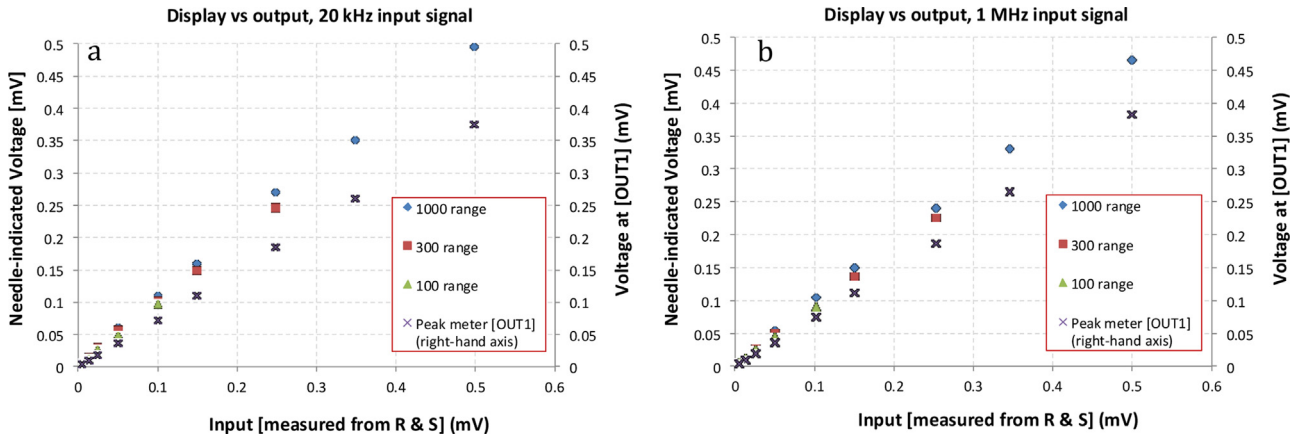

Fig. 2. Linearity and loading effect of the cavitometer as determined by comparing the needle display with the output from unit connected to the URE-3 meter during direct signal injection, for (a) 20 kHz and (b) 1 MHz. The legend shows the sensitivity ranges selected in the cavitometer unit (see Fig. 1a).

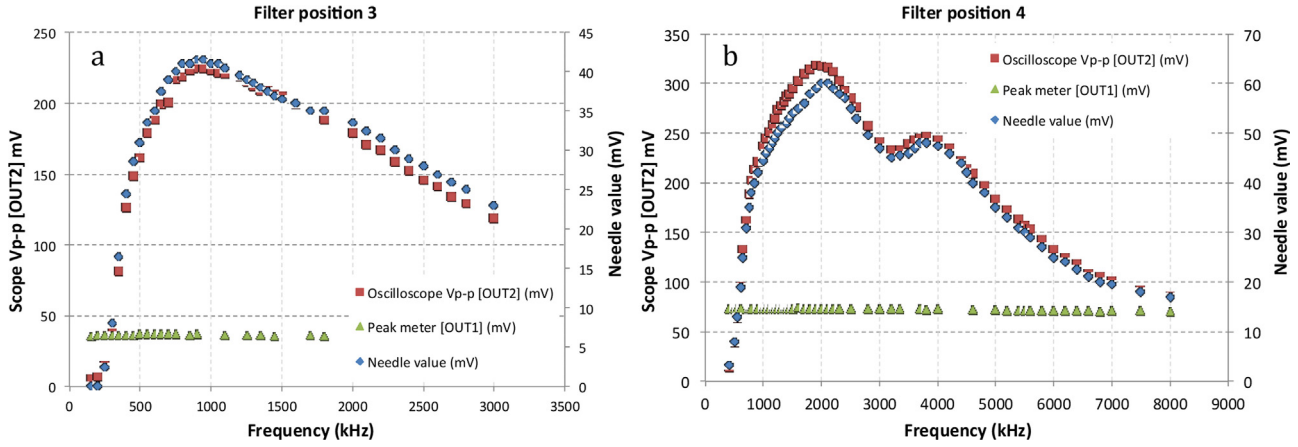

Fig. 3. Frequency response of the filtered OUT 2 channel and the needle display for two filter positions at (a) 3 and (b) 4 (see switch activity in Fig. 1a). OUT 1 output remains unaffected across the entire spectrum, as expected.

shown in Fig. 1b. The probe tip was then located 15 mm away from a standard NPL source operating in the range 17–21 kHz (typical of sonotrodes used in fluid processing), and the resulting signal from OUT 1 was displayed and recorded on a Picoscope 4424 (Pico Technology, St. Neots, UK). Then, a reference calibrated NPL hydrophone was placed in the same field location (within ±0.5 mm), and the waveform was acquired using the same procedure. By comparing the signal amplitudes, and with the knowledge of the sensitivity of the reference hydrophone, the sensitivity of the cavitometer probe was obtained. At the frequencies of interest, calibration figures were derived as shown in Fig. 4 (the inherent uncertainty is ±20% in each case). Note that the changes in the sensitivity levels with frequency are most likely due to the mechanical design of the cavitometer probe [32].

The sensitivity of the cavitometer hydrophone at frequencies characteristic of emissions from bubbles undergoing inertial cavitation was also investigated at NPL.

The device was set up vertically, and calibrated using NPL's multiple frequency substitution technique based on non-linear distortion of an initially sinusoidal 1 MHz tone burst [33]. The probe was also calibrated in an inclined position at an angle of 35° to the vertical, as this was the likely deployment in subsequent sonotrode measurements. Results showed that at 1 MHz, the calibrated sensitivity is 0.15 nV/Pa on average for both positions (vertical and inclined). The reason for such a low sensitivity value is likely to be due to the high acoustic absorption coefficient of the tungsten waveguide and the fact that this probe is designed for viscous and high temperature environments where activity from the cavitation bubbles is more powerful [32].

The sensitivity is averaged over four measurements, and has uncertainty of ±20%. This is composed of the statistical variation over the four averages, temperature variations, and spatial averaging of the acoustic field over the side-on configuration (the receiving element is comparable in size to the wavelength at 20 kHz) [33].

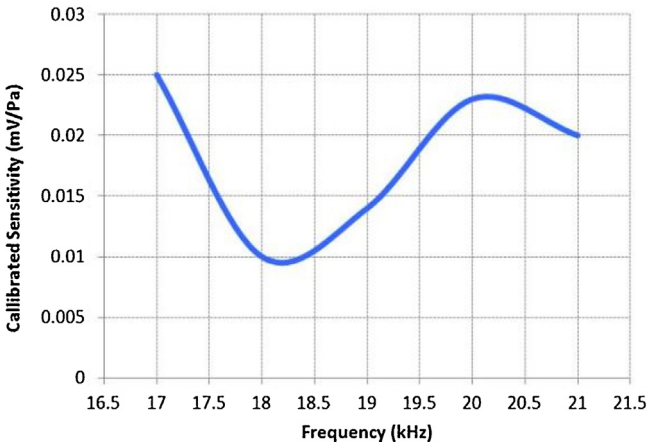

Fig. 4. Derived sensitivity of the cavitometer probe for the low frequency spectrum.

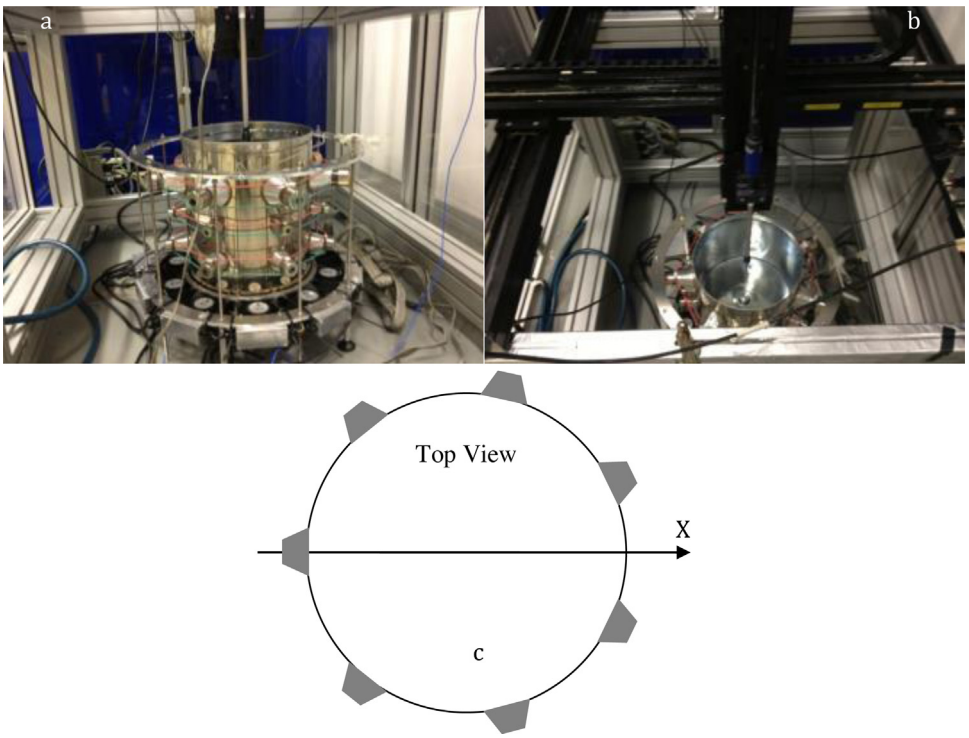

Fig. 5. Experiments of cavitometer probe spatial sensitivity: (a) the reference multifrequency cavitation vessel at NPL, (b) the cavitometer probe submerged along the centre axis of the vessel, and (c) the orientation of the cavitomer hydrophone scans.

3.2.2. Spatial resolution

To investigate the spatial sensitivity and the temporal repeatability of the cavitometer, it was deployed in the multi-frequency cavitation reference vessel at NPL [34]. This vessel is shown in Fig. 5 and comprises a 14 L cylindrical water tank of approximately 200 mm in diameter, around which 21 transducers are attached, arranged in three rows each of seven devices. For the purposes of this study, tests were carried out using only the upper transducer row at a driving frequency of 21 kHz, over four transducer drive voltage levels. This generates an acoustic pressure distribution within the water volume with regions of locally intense cavitation, and also areas where no cavitation occurs [34].

X-direction scans (2 mm step size, submersion depth 76 mm) are shown in Fig. 6 for cavitometer settings "HYDR" and "4" associated with low- and high-frequency detection respectively (see Fig. 1a). The consistency in the OUT 1 plots (Fig. 6a and c) shows the stability and repeatability of the cavitometer hydrophone in detecting the lower frequency signal (which is dominated by the 21 kHz component). These figures are effectively measurement repeats and show good agreement with each other, as would be expected. More prominent structure is seen at the higher drive levels (0.1 and 0.2 V), with the levels of the subsidiary maxima relative to the central lobe increasing. Additionally, peaks at 50 mm and 100 mm suggest locations where off-axis cavitation activity could occur. The OUT 2 variation (Fig. 6b and d) shows that the level and spatial distribution of the measured signals changes as the "Activity" filter is changed from "HYDR" to setting "4". As described earlier (see Table 1), this is because the filter bandwidth increases with increasing filter number so that the ICA-3HT box displays and outputs only the acoustic signals corresponding to cavitation, which are significantly lower in level. Thus, it is clear that the OUT2 channel provides full bandwidth detail, but varies as intended with filter setting. Fig. 6d shows that the setting 4 bandwidth (up to 2.5 MHz) picks up a different spatial variation than the direct field (Fig. 6b), demonstrating that the acoustic pressure threshold is only exceeded over a significant proportion of the scan for the 0.2 V drive setting.

The slight changes in the shape of the structures with the different settings in OUT 1 are assumed to be related to the stochastic nature of the inertial cavitation process, to small changes in position of the cylindrical focus within the vessel, or possibly to small movements of the cavitometer probe when positioned at the centre of the vessel due to the strong radiation forces produced by the transducers.

3.2.3. Spatial variation of cavitation activity

To characterise the cavitometer hydrophone in terms of its ability to resolve the spatial variation in cavitation, another set of measurements was conducted by comparing it with it to the NPL Cavisensor [28,29]. The Cavisensor, which has been designed for quantifying the degree of cavitation activity, passively responds to acoustic emissions generated by the cavitation bubbles, with a high degree of spatial resolution, endowed by its selectively-shielding design: any acoustic signals detected at 1 MHz and above arise from cavitation events occurring within the cylindrical body of the cavitation sensor.

Tests were conducted only for "Activity" setting "3" of the ICA-3HT device, a setting at which the total cavitation activity is captured; and for the Cavisensor, integrating the broadband acoustic emission over the range 1.5–7.0 MHz. Comparing the trends in Fig. 7 shows quite good qualitative agreement between the two devices. The measured voltage levels for the Cavisensor are significantly greater, because of its design: the tungsten waveguide in the cavitometer attenuates the received signal amplitude. The Cavisensor resolves more detail in the central peak, for the three highest drive levels, suggesting that by comparison, the cavitometer hydrophone spatially averages the signals it measures over a wider region, although it is integrating over a wider bandwidth. For the 0.1 V drive setting, the cavitometer measurements suggest that inertial cavitation occurs across the vessel, whereas it appears more localised for the Cavisensor. Overall, this suggests that the effective spatial resolution of the Cavisensor is better than that of the cavitometer probe, where it is estimated to be of the order of

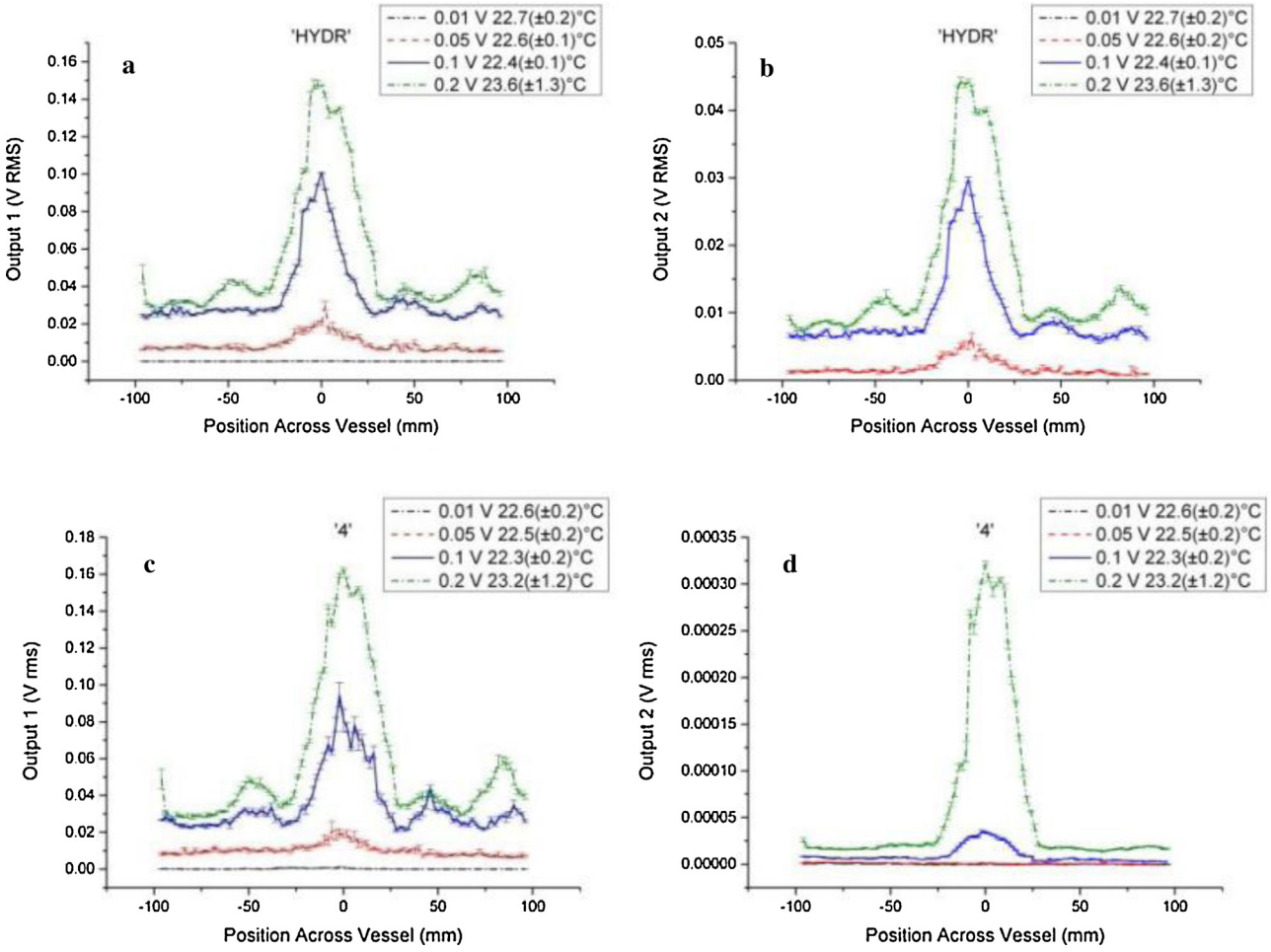

Fig. 6. Average variation of the cavitation activity with *x*-axis position across the reference cavitation vessel at 4 different drive settings, 0.01, 0.02, 0.1 and 0.2 V determined using the cavitometer probe submerged at 76 mm depth using (a, c) OUT 1 and (b, d) OUT 2 channels, and two filter settings ("HYDR" and "4").

40–50 mm. Understanding spatial resolution (the ability of a sensor to resolve the detail of cavitation within the volume under test) is important as it allows characterisation and hence scale-up of cavitating systems, with a good understanding of effective treatment volumes. Taking into account that treated volumes are large, the obtained spatial resolution of the cavitometer is adequate. Note that the cavitometer probe differs from a typical hydrophone, as it has a long cylindrical receiving element, which clearly means it spatially averages over a wider reception volume in the cavitating fluid.

3.2.4. *Spatial sensitivity*

The exposed section of the tungsten waveguide is about 11 cm long (see Fig. 1b). This surface is potentially sensitive to cavitation signals received over a wide area, as seen from the previous tests (Fig. 7), and in practice may result in significant spatial averaging. To test this effect, a small-beam ultrasonic transducer was set up to

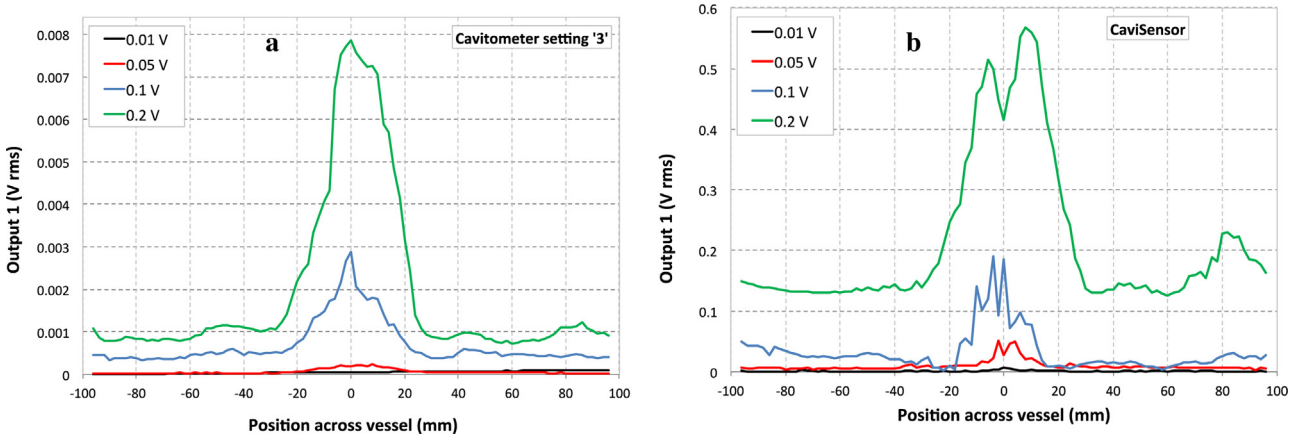

Fig. 7. X-direction axial scans at applied power levels of 0.01, 0.02, 0.1, 0.2 V for (a) cavitometer hydrophone and (b) Cavisensor at 76 mm depth.

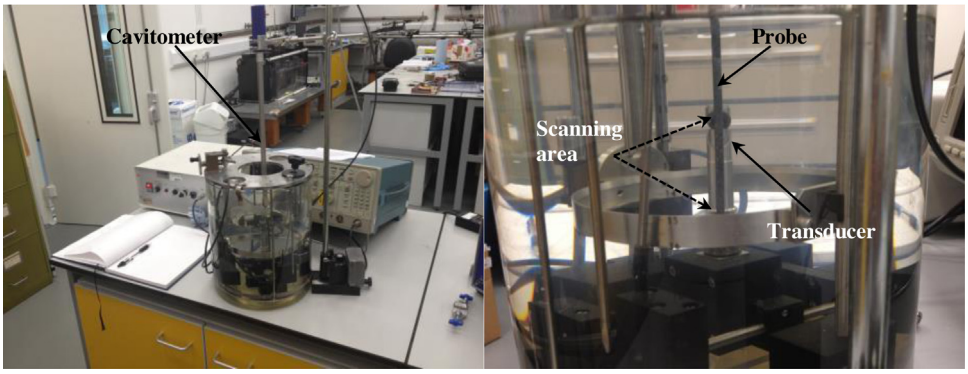

Fig. 8. Small beam transducer used to examine spatial sensitivity of the cavitometer probe at MHz frequencies (a) experimental set-up and (b) scanning area of the probe (enlarged from (a)).

examine the variation in the cavitometer probe response as a function of position along the tungsten waveguide as shown in Fig. 8. This was achieved by using a vertical positioning rig, in which a sideways-looking transducer emitted signals towards the exposed part of the probe at a frequency around 5 MHz (typical of high frequency emissions from inertial cavitation) from a distance of 20 mm, and then scanned vertically. The cavitometer OUT 1 channel was monitored using the URE-3 voltmeter. Analysis was performed only in the middle-lower part of the probe starting at 5 mm from the probe's tip, as this region was used beneath the sonotrode in later tests. Results are shown in Fig. 9 for three repeated measurements (A–C), with the cavitometer probe rotated through 180° about its cylindrical axis. Ad hoc checks at 90° and 270° rotation showed similar results to the 180-° position.

The test shows that there is a variation of around 15% in the probe sensitivity over its length, and a suggestion (at the 5 MHz frequency) of some periodicity, and hence most likely of structural resonances in the probe response. The impact of this on actual measurements of cavitation is complex. If the tungsten tip is fully-immersed, this variation could be considered as an uncertainty contribution, but only if the incoming signal interacts with the tungsten tip uniformly, which is unlikely in practice. For partial immersion, particularly for the probe positioned at an angle, the measured signal can be considered to be averaged over the part of the tungsten probe, e.g. in the region 5–17 mm from Fig. 9 (due to the limitations of the setup it was not possible to apply the driving signal to the very tip of the probe, i.e. the 0 mm position). Assuming that cavitation signals may arrive at the probe from all sides, the average received signal over this region, taken from the two graphs, is 4.95 mV with a standard uncertainty of 2%. Hence, 2% is used as an uncertainty contribution for this aspect of the overall cavitometer hydrophone sensitivity.

4. Calculating acoustic pressures

Comparison of the measurements obtained using the cavitometer with the measurements from the calibrated NPL hydrophone allows conversion of the measured values to acoustic pressure. At each frequency of interest, the voltage output of the cavitometer (mV) can be then translated into an acoustic pressure value (Pa) according to Eq. (1). For the higher frequencies (MHz), there is an uncertainty of 2% as previously discussed for the spatial sensitivity, plus we assumed, based on the previous NPL experience, an inherent uncertainty of 20% in the probe calibration itself resulting from the robust design required for the high-temperature measurements. Other factors that should also be taken into account include the considerable uncertainty in transferring a calibration performed at ambient temperature in water to molten Al at 700–750 °C.

$$\frac{V}{S} \pm Er = P \tag{1}$$

where V is the voltage output (mV), S is the spatial sensitivity, Er is uncertainty of calibration, and P is the RMS acoustic pressure (Pa).

The raw analogue voltage amplitude (mV) is received from OUT 1 in the ICA-3HT device and is then converted into a digital form using a standard oscilloscope device. Consequently, the component of the signal at the frequency of interest is isolated from a Discrete Fourier transform of the signal. Eq. (1) is then applied to convert the voltage to RMS acoustic pressure values at the frequency of interest. Therefore, the acoustic pressures that are measured by the cavitometer probe as a function of frequency provide physical meaning to the measured results. Calculated pressures must be treated with some caution, however, as the original calibrations were performed under non-cavitating conditions; but are considered suitable as a

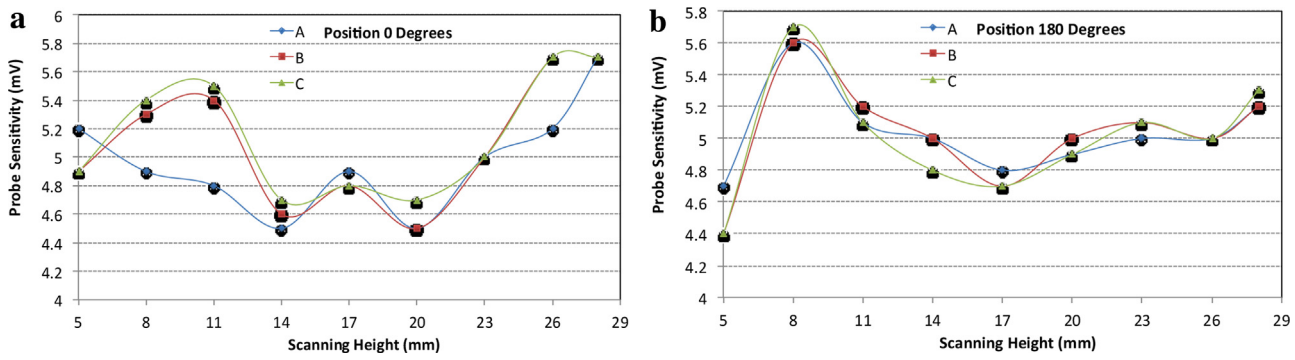

Fig. 9. Probe sensitivity as measured using the experimental setup of Fig. 8 for positioning of the probe in relation to the transducer at (a) 0° and (b) 180°. Three independent measurement runs (A–C) were carried out.

first step in placing the cavitometer measurements in the context of real physical values.

5. Experimental results

5.1. Cavitation intensity measurements

For these series of tests, the cavitometer probe was set up inside a small 3-L tank containing filtered (95%, 5 μm) deionised water. A 20 kHz Sonic System P100 with a 15 mm diameter sonotrode tip able to produce tip displacement amplitudes up to 44 μm (p–p) was placed in the centre of the tank and the cavitometer probe was vertically positioned at 93 mm from the sonotrode tip, with the Cavisensor equidistant on the other side of the sonotrode, to monitor the cavitation activity as shown in Fig. 10 and explained in Section 5.2. All devices were submerged to a depth of 20 mm.

On each of the graphs in Fig. 11, a range of measured values is shown, together with a mean. Measurements were made as a function of sonotrode tip displacement amplitude using the OUT 1 and the OUT 2 channels of the ICA-3HT device as depicted in

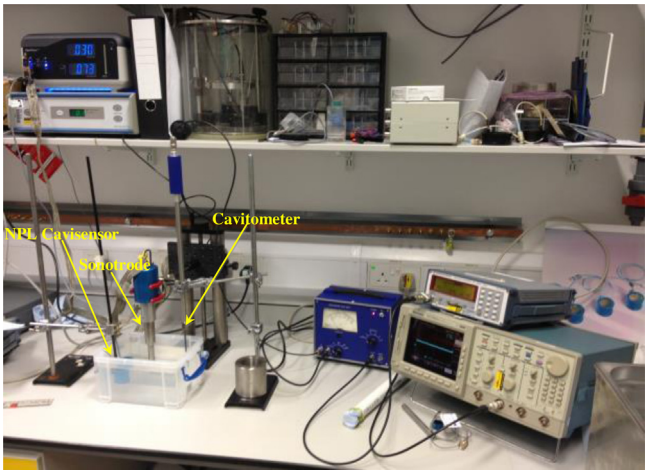

Fig. 10. Experimental setup used for measuring cavitation activity for different nominal applied power of the acoustic transducer.

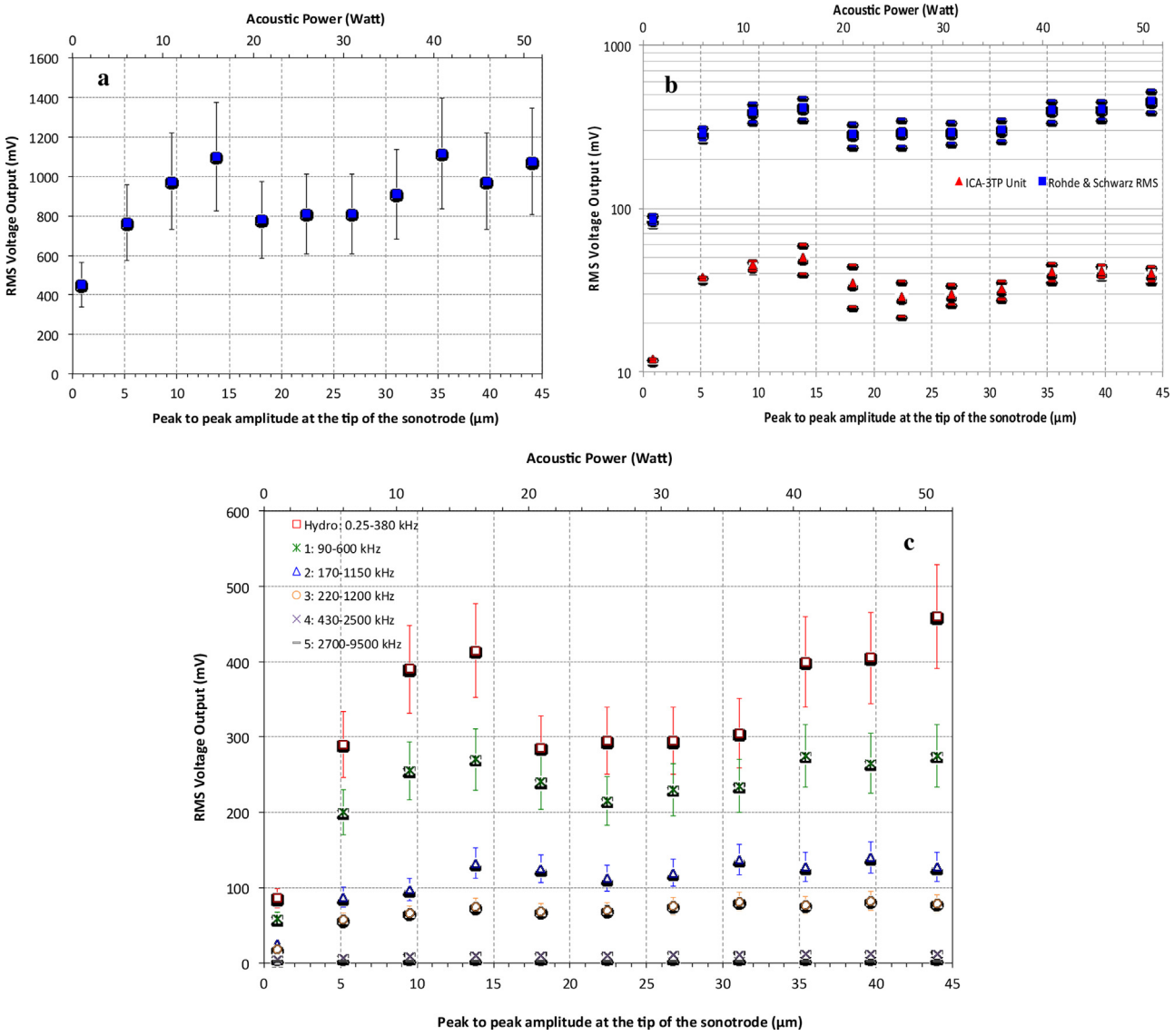

Fig. 11. (a) Change of the voltage output as a function of sonotrode tip displacement measured with a Rohde–Schwarz URE-3 RMS connected to OUT 1; (b) logarithmic scale of voltage output measurements taken using the needle meter of the ICA-3HT device and the Rohde-Schwarz URE-3 RMS device attached to OUT 2; and (c) cavitation intensity against the acoustic power measured with a Rohde–Schwarz URE-3 RMS for the different filter settings of the ICA-3HT OUT 2 channel.

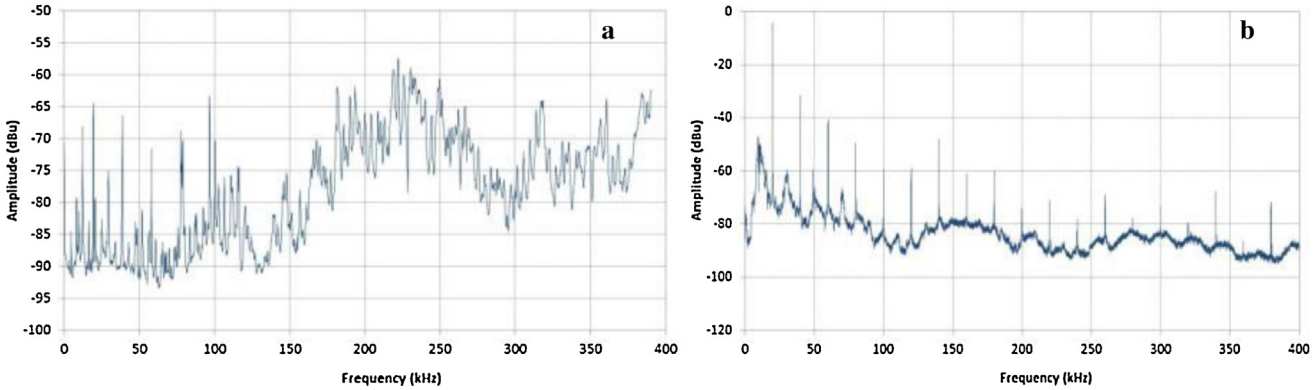

Fig. 12. Example of acoustic spectrum generated by a 20 kHz ultrasonic transducer with (a) p–p amplitude of 8.5 μm in water captured using a cavitometer probe and (b) Cavisensor.

Fig. 11. In Fig. 11a, the raw signal derived from the cavitometer probe captured using OUT 1 connected to the URE-3 device is given. This shows the variation of the probe output with different power levels, which will be dominated by the direct field component at 20 kHz. There is an initial rise in the values up to 15 W followed by a reduction and then a further increment. This drop in the curve at 15 W is associated with the shielding and scattering effects commonly generated in sonicated environments. As the acoustic pressure increases, it is highly likely that cavitation shielding is occurring, when the bubbly cloud produced immediately in front of the radiating surface of the sonotrode limits the sound wave propagation and associated peak pressures achievable in the tank. The same graphical pattern (scaled) is also observed in Fig. 11b showing the results measured only for the "HYDR" setting using the displayed value (needle meter) of the ICA-3HT device and by the URE-3 connected to OUT 2.

Cavitation intensity was also measured for each of the cavitometer filter settings as shown in Fig. 11c where only the corresponding OUT 2 values (determined using the URE-3 device) are shown. Clearly, the variation of measured cavitation, regardless of filter setting or device, is not linear with drawn power and follows a similar pattern to Fig. 11a and b, showing the expected relationship between direct field and resulting cavitation. There is a small change in curve shape as a function of power when the different frequency filters are compared, but within the signal variations seen, this is not significant, suggesting that even at low drive levels significant inertial cavitation is generated by the sonotrode. Using the OUT 2 signal, rather than relying on the needle display of the ICA-3HT, clearly provides greater measurement fidelity due to the higher signal-to-noise levels, such that the voltmeter is still able to distinguish variations in cavitation as a function of applied power for filter settings 4 and 5. This strongly suggests that OUT 2 provides the best-refined measurement channel, when the cavitometer is used as a signal processing unit to distinguish cavitation signals from direct field signals. However, for obtaining acoustic pressure values, the unfiltered signal measurements from OUT 1 (monitored using the Picoscope 4424) are used from here onwards, for acquisition and signal processing using the calibration data described earlier in this paper.

5.2. Comparison of the cavitometer with the Cavisensor

The acoustic spectra for water, as received by the cavitometer and by the Cavisensor during experiments similar to those in Fig. 10, are shown in Fig. 12. In this case, the cavitometer probe was placed in the cavitation zone below the sonotrode at a 35 degrees angle while the Cavisensor accommodated the tip of the sonotrode inside its aperture. The prominent fundamental frequency component (20 kHz) is clearly present in both graphs, with further contributions from sub- and ultra-harmonics frequencies. The Cavisensor resolves the frequency peaks better than the cavitometer: this is expected since it was designed specifically for measurements in water while the cavitometer has been designed for operation in liquid aluminium. However, the significant 'hump' located in the 200 kHz region by the cavitometer cannot be attributed to intense cavitation activity at these frequencies, but rather as an artefact of the cavitometer. This may be due to the variation of the cavitometer sensitivity with frequency, or to internal mechanical vibrations of the cavitometer probe as it uses a long waveguide [32].

To investigate the cavitation activity in more detail, the corresponding voltage outputs were recovered from the spectra in Fig. 12 by an inverse Fast Fourier Transform (FFT). The two sensors were compared in the low and high frequency ranges.

In Fig. 13 a generalised approach of the voltage output (cavitation intensity) for different vibration amplitudes of the sonotrode is shown by the normalization to the maximum value. Fig. 13 presents the inverse FFT data of Fig. 12 normalized to the maximum value for the respective sensors. This was achieved by dividing each of the measured values with the maximum measured value among all the variables. For example, the voltage output in each case was divided by the maximum voltage output so a unit-based normalization to the maximum value was achieved. In this way, all the experimental variables from these set of experiments are related, giving meaningful generalised results.

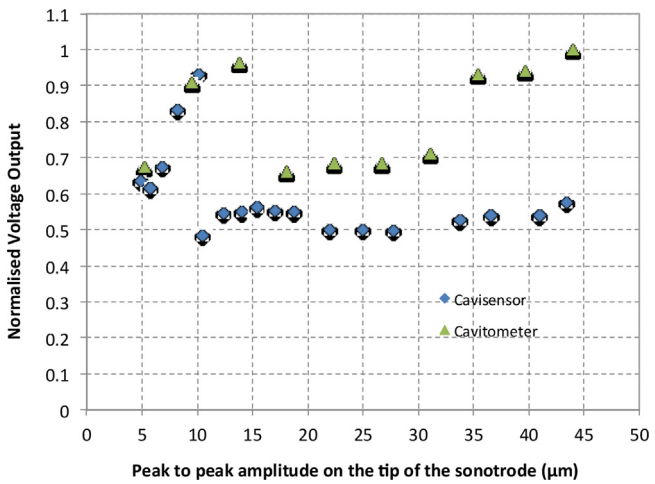

Fig. 13. Comparison of the direct field (20 kHz) between two different sensor devices: the cavitometer (Fig. 12a) and the Cavisensor (Fig. 12b).

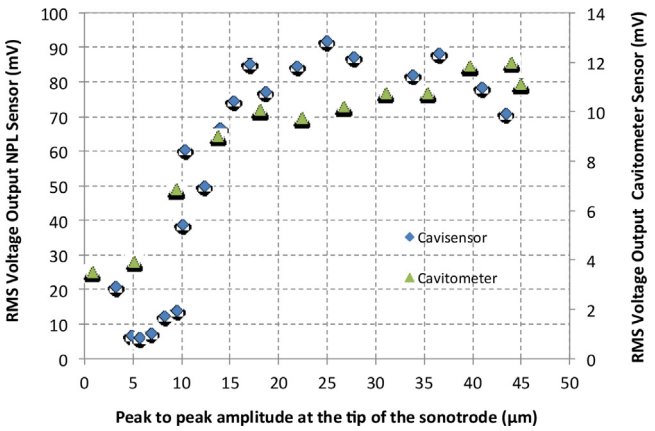

Fig. 14. Comparison of cavitation activity (progression of inertial cavitation) as a function of the tip amplitude between the Cavisensor (filtered from 1.5 to 7 MHz) and the cavitometer (filter setting "4" range: 0.4–2.5 MHz).

Reasonable agreement was achieved when the direct field was evaluated for both sensors, as shown in Fig. 13. There is an upward progression of the voltage for radiating surface displacements up to 10–15 μm, and then a significant drop due to the cloud shielding effect, which limits the penetration of the driving field into the liquid. After this point, the Cavisensor exhibits a stable trend: staying unaffected by the increment of tip amplitude from the transducer. This behaviour suggests that shielding perhaps gets more prominent, but also, the progressive transfer of energy from the direct field frequency to broader bands, demonstrating the non-linearity of acoustic signals in a transient cavitation regime. In contrast, the cavitometer shows a steady increase in the output voltage with increasing the amplitude larger than 30 μm. It is likely that differences in the cavitometer and Cavisensor designs and geometrical features result in a broader locus of signals received by the cavitometer from many different places across the vessel, whereas the Cavisensor is more localised.

The plots in Fig. 14 show the progression of inertial cavitation with the nominal applied power. The measured cavitation activity as a function of tip amplitude was compared for the two sensors. The MHz dataset from the Cavisensor was high-pass filtered, discarding the information below 1.5 MHz. This filtered signal was then compared with the cavitometer signals for filter setting 4 that registered the emissions from cavitation bubbles, see Table 1. After a period of rapid increase, in the driving field region just beyond the cavitation threshold, the values stabilize at around 15 μm p–p displacement and then continue with small fluctuations until the maximum amplitude is reached. Note the highly nonlinear behaviour: the three-fold increase in peak-to-peak amplitude corresponds to a similar increase in drawn power, yet the resulting measured cavitation increases by just 25%. This is likely to be attributable to shielding effects, as noted above, and the increasing inefficiency of energy transfer to the liquid by the sonotrode (decoupling). The apparently greater dynamic range of the Cavisensor is likely to be due to the greater overall bandwidth measured (1.5–7 MHz, vs 0.3–2.5 MHz for the cavitometer on filter setting 4, see Table 1), plus its inherently higher sensitivity, described in Section 3.2.3.

The small differences in the compared sensor outputs with tip amplitude plots are likely to be due to the volume of the fluid over which the sensor responds. For the cavitometer, the spatial resolution was estimated to be around 40–50 mm while for the Cavisensor it is about 4 mm. This implies that the cavitometer output (for cavitation activity) is expected to be more stable as a function of the tip amplitude, as it probably detects signals over a wider locus of points. In general, the results are in a good agreement between the two tested devices implying that the cavitometer is also able to measure non-linear cavitation emissions from bubbles' activity at high frequencies (MHz) for water.

5.3. Preliminary acoustic pressure measurements in liquid Al

To investigate the pressure characteristics of the acoustic field in molten aluminium (Al), a preliminary study was conducted: to the authors' knowledge, this is the first time such a measurement has been carried out. These experiments demonstrate the importance of the performed work of cavitometer calibration to the sonochemical and metallurgical applications. Pure Al was selected as a material for comparison because it is readily castable, extensively studied, and widely used in metallurgical, automotive, and aerospace industry as an alloy component. Additionally, Al and water liquid phases have close kinematic viscosities while their Newtonian behaviour is similar [35] making water a frequently used candidate in physical modelling of liquid Al. A charge of 5.2 kg of Al was introduced in a 15 cm diameter and 18 cm deep clay-graphite crucible, with the inside coated with boron nitrate (BN). The Al charge was melted in an electric furnace, with the melt temperature adjusted to 760 °C. The ultrasonic equipment consisted of a 5-kW generator and a 5-kW water-cooled magnetostrictive transducer (Reltec, Russia). The sonotrode consisted of a Ti concentrator and Nb tip driven by a transducer that oscillates at a nominal fundamental frequency of 17.5 kHz producing a peak-to-peak amplitude of 39 μm at 3.5 kW acoustic power inside the liquid melt. Note that this type of ultrasonic transducers is designed to maintain the maximum input power rather than the oscillation amplitude. The sonication was performed by dipping the Nb tip (sonotrode) from the top of the melt to a depth of approximately 5 mm. The tip was preheated and the melt temperature was controlled during the process. There was no controlled atmosphere. The melt temperature is measured by a K-type thermocouple. Test configurations and the different positions of the cavitometer probe during the measurements are shown schematically in Fig. 15.

Line scan measurements across the *x*-axis of the vessel were performed by placing the cavitometer (submersion depth of the cavitometer probe about 7 cm) at 3 different positions inside the melt (i) near the sidewall (ii) between the sidewall and the sonotrode (half-radius of the crucible) and (iii) below the sonotrode at an angle of 35°. A typical acoustic spectrum for liquid Al, as received by the cavitometer, is shown in Fig. 16a. The spectrum plot is comparable to that of the water (Fig. 12a) further reinforcing the existing views [35] that water and Al share similar behaviour under ultrasonic treatment. Specifically, the fundamental frequency component (f_0) at 17.5 kHz is apparent with further contributions from sub- and ultra-harmonic frequencies.

For reproducibility, the FFT plots, as exemplified by Fig. 16a, are the average of 30 signal measurements each. The acoustic pressure is calculated from the spectral line at the nominal frequency of the sonotrode. The errors in the acoustic pressures are obtained from a Student test analysis of the 30 measurements.

With the assumption that the calibration of the cavitometer probe in water is directly transferable to the conditions encountered in molten Al, the scan data can be used to estimate RMS pressure values. In Fig. 16b, acoustic pressures in the range of the driving frequency f_0 are less than perhaps expected, given that cavitation occurs at this sonotrode power [21]. The reason for this maybe the absorption of acoustic energy by the bubbly environment. The drop in acoustic pressure can easily reach 90% if the cavitation index (volume fraction of bubbles in the cavitation zone) is above 0.2 [36]. It is also possible that energy accumulates within long-lived Al cavitation bubbles as seen by the recent X-ray imaging results in [37], and is subsequently released back to the liquid volume by non-linear activity at higher frequencies, in a

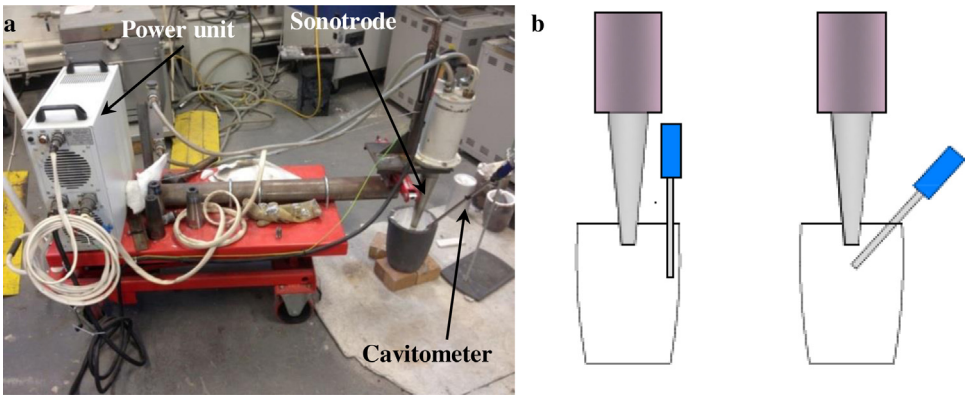

Fig. 15. (a) Experimental test rig for molten Al (b) a scheme showing positions of the cavitometer: near the side wall at 7 cm from the sonotrode and directly under the sonotrode at an angle of 35° (measurements were also performed at half-radius, not shown here).

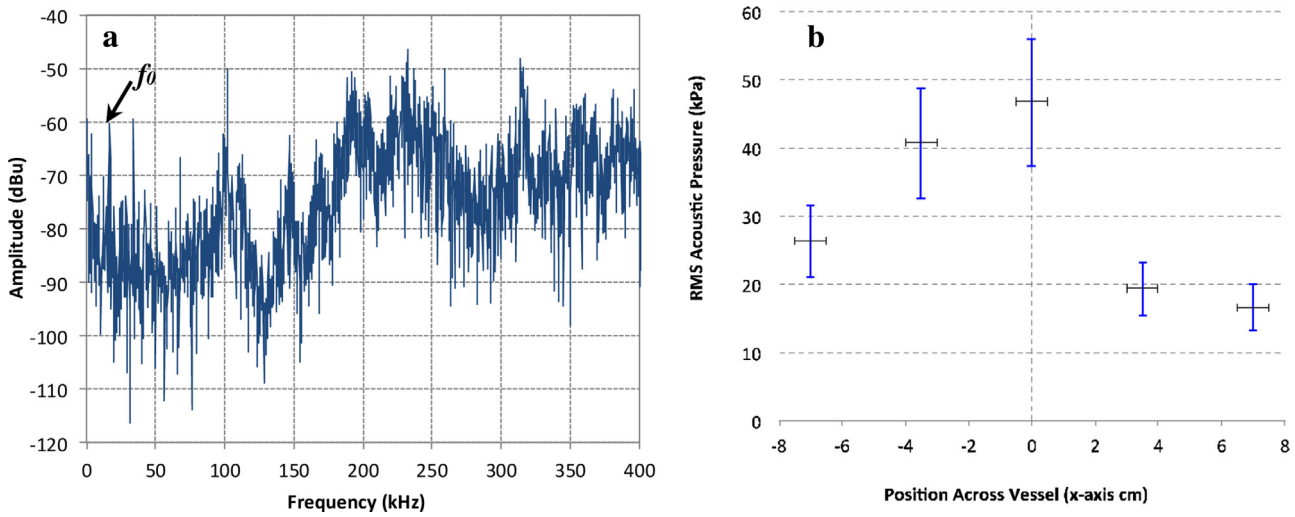

Fig. 16. (a) Typical example of acoustic spectrum generated by the magnetostrictive ultrasonic transducer at 17.5 kHz driving frequency and measured with the cavitometer tip positioned about 3–4 cm below the sonotrode's tip surface. (b) Variation in RMS acoustic pressure of the driving frequency with *x*-axis position across the cylindrical vessel.

form of long-duration stable cavitation as explained in [38]. Recent experimental measurements using the cavitometer showed that the attenuation of high-frequency emissions is greater in liquid aluminium as compared to water [39].

It is also seen in Fig. 16b that the pressure field distribution is not completely symmetrical. Specifically, across the negative *x*-axis line scan, pressures were found to be about 50% higher than at the corresponding locations in the positive *x*-axis. The reason for this acoustic pressure fluctuation could be attributable to the stochastic nature of the cavitation phenomenon and to the displacement of the focused point of the cone-like streamer when is disturbed by turbulent fluid currents [40]. Consequently, acoustic energy is projected towards the direction of the divergence increasing the pressure locally.

6. Conclusions

This paper describes a series of systematic studies undertaken to calibrate and assess the performance of a new cavitation sensor, called a high-temperature cavitometer, used for quantifying the degree of cavitation activity occurring in high temperature sonicated liquids such as molten metals. Furthermore, a comparative study using the established broadband NPL Cavisensor was conducted, for measurements in water. Key findings of the study are:

1) The cavitometer is a robust, sensitive, stable and repeatable device (at MHz frequencies which correspond to cavitation emissions, to around 20% reproducibility, which is of a similar order to commercial hydrophones).
2) It is capable of detecting signals up to 9.5 MHz despite the limitations due to its waveguide-based metal design (required for high-temperature operation).
3) The cavitometer was calibrated as a hydrophone in the range of 17–21 kHz and at 1 MHz, which enables it to be used for estimating acoustic pressures of the direct field as well as of the continuum broadband component associated with inertial cavitation.
4) Its outputs have an impedance loading effect of 30% at low frequencies and 20% at high frequencies. These should be accounted for when using the device for any acoustic measurements.
5) The cavitometer has an estimated spatial resolution of 40–50 mm, and can therefore be used to monitor the broadband acoustic emissions generated by bubbles undergoing acoustic cavitation within molten metals.
6) The spatial sensitivity of the tungsten probe tip along its length shows variations corresponding to an uncertainty of ±2%. This should be accounted for when the device is used for acoustic measurements at MHz frequencies (alongside other sources such as the inherent uncertainty of the probe).

7) Comparison between the Cavisensor and the cavitometer showed consistency during monitoring cavitation activity both in the narrow (direct field/stable cavitation) and in the broadband spectrums (cavitation bubbles/transient cavitation) implying the suitability of the cavitometer to measure acoustic emissions.
8) Acoustic pressure measurements within a liquid aluminium (Al) volume were performed, for the first time. The measured RMS acoustic pressures were found to be up to 50 kPa at the driving frequency f_0.

The calibrated cavitometer will allow us to develop standardized methods for (a) quantifying the degree of acoustic cavitation, (b) determining the limits of the cavitation region and (c) characterising acoustic pressure fields occurring within extreme liquid environments. Thus, calibration of the specific cavitometer is likely to hold the key to the optimization of many ultrasound-driven sonochemical and metallurgical applications as considerable insight and fundamental understanding of the cavitation activity will be necessary when attempting to scale-up processes from laboratory bench to industrial plant. Eventually, the cavitometer can be established as a standardised quantitative tool for measuring cavitation activity in liquid metals.

Acknowledgements

This work is performed within the Ultramelt Project supported by the Engineering and Physical Sciences Research Council (EPSRC) Grants EP/K005804/1 and EP/K00588X/1.

References

[1] T.G. Leighton, The Acoustic Bubble, Academic Press, London, 1994.
[2] J.R. Laguna-Camachoa, R. Lewis, M. Vite-Torres, J.V. Mendez-Mendez, A study of cavitation erosion on engineering materials, Wear 301 (2013) 467–476.
[3] I. Tzanakis, W.W. Xu, D.G. Eskin, P. Lee, N. Kotsovinos, In situ observation and analysis of ultrasonic capillary effect in molten aluminum, Ultrason. Sonochem. 27 (2015) 72–80.
[4] C.C. Coussios, R.A. Roy, Applications of acoustics and cavitation to noninvasive therapy and drug delivery, Annu. Rev. Fluid Mech. 40 (2008) 395–420.
[5] W. Lauterborn, E. Cramer, On the dynamics of acoustic cavitation noise spectra, Acustica 49 (1981) 280–287.
[6] V.I. Ilyichev, V.L. Koretz, N.P. Melnikov, Spectral characteristics of acoustic cavitation, Ultrasonics 27 (1989) 357–361.
[7] M. Hodnett, R. Chow, B. Zeqiri, High-frequency acoustic emissions generated by a 20 kHz sonochemical horn processor detected using a novel broadband acoustic sensor: a preliminary study, Ultrason. Sonochem. 11 (2004) 441–454.
[8] G.J. Price, M. Ashokkumar, M. Hodnett, B. Zeqiri, F. Grieser, Acoustic emission from cavitating solutions: implications for the mechanisms of sonochemical reactions, J. Phys. Chem. B 109 (2005) 17799–17801.
[9] B. Avvaru, A.B. Pandit, Oscillating bubble concentration and its size distribution using acoustic emission spectra, Ultrason. Sonochem. 16 (2009) 105–115.
[10] R. Esche, Untersuchung der Schwingungskavitation in Fliissigkeiten, in: Acustica, 2, Akust. Beih, 1952, pp. AB208–AB218.
[11] N.V. Dezhkunov, A. Francescutto, F. Calligaris, A.L. Nikolaev, The evolution of a cavitation zone in a focused ultrasonic field, Tech. Phys. Lett. 40 (2014) 732–735.
[12] T. Colonius, F. D'Auria, C.E. Brennen, Acoustic saturation in bubbly cavitating flow adjacent to an oscillating wall, Phys. Fluids 12 (2000) 2752–2761.
[13] B. Osgood, The Fourier transform and its applications, lecture notes EE 261 distributed in Electrical Engineering Department at Stanford University, USA, (2007).
[14] K. Yasui, Temperature in multibubble sonoluminescence, J. Chem. Phys. 115 (2001) 2893–2896.
[15] D.J. Flannigan, S.D. Hopkins, C.G. Camara, S.J. Putterman, K.S. Suslick, Measurement of pressure and density inside a single sonoluminescing bubble, Phys. Rev. Lett. 96 (2006) 204301.
[16] C.E. Wang, Brennen, The noise generated by the collapse of a cloud of cavitation bubbles cavitation and gas–liquid flow in fluid machinery devices, ASME 226 (1995) 17–29.
[17] R.E. Apfel, Acoustic cavitation, in: P.D. Edmonds (Ed.), Methods of Experimental Physics, vol. 19, Academic, London, 1981, p. 355.
[18] M. Ashokkumar, M. Hodnett, B. Zeqiri, F. Grieser, G.J. Price, Acoustic emission spectra from 515 kHz cavitation in aqueous solutions containing surface-active solutes, J. Am. Chem. Soc. 129 (2007) 2250–2258.
[19] D.G. Eskin, K. Al-Helal, I. Tzanakis, Application of a plate sonotrode to ultrasonic degassing of aluminum melt, J. Mater. Proc. Technol. 222 (2015) 148–154.
[20] T.V. Atamanenko, D.G. Eskin, L. Zhang, L. Katgerman, Criteria of grain refinement induced by ultrasonic melt treatment of aluminum alloys containing Zr and Ti, Metall. Mater. Trans. A 41 (2010) 2056–2066.
[21] G.I. Eskin, D.G. Eskin, Ultrasonic Treatment of Light Alloy Melts, second edition, CRC Press, Boca Raton, 2014.
[22] M. Keswani, S. Raghavan, P. Deymier, Electrochemical investigations of stable cavitation from bubbles generated during reduction of water, Ultrason. Sonochem. 21 (2014) 1893–1899.
[23] J. Campbell, Effects of vibration during solidification, Intern. Met. Rev. 2 (1981) 71–108.
[24] E.A. Heidemann, Metallurgical effects of ultrasonic waves, J. Acoust. Soc. Am. 26 (1954) 831–842.
[25] K.S. Suslick, Y. Davidenko, M.M. Fang, et al., Acoustic cavitation and its chemical consenquences, Phil. Trans. R. Soc. Lond. A 357 (1999) 335–353.
[26] S. Komarov, K. Oda, Y. Ishiwata, N. Dezhkunov, Characterization of acoustic cavitation in water and molten aluminium alloy, Ultrason. Sonochem. 20 (2013) 754–761.
[27] H. Huang, D. Shu, Y. Fu, J. Wang, B. Sun, Synchrotron radiation X-ray imaging of cavitation bubbles in Al–Cu alloy melt, Ultrason. Sonochem. 21 (2014) 1275–1278.
[28] B. Zeqiri, P.N. Gelat, M. Hodnett, N.D. Lee, A novel sensor for monitoring acoustic cavitation, part I: concept, theory and prototype development, IEEE Trans. Ultrason. Ferroelectr. Freq. Control 50 (10) (2003) 1342–1350.
[29] B. Zeqiri, N.D. Lee, M. Hodnett, P.N. Gelat, A novel sensor for monitoring acoustic cavitation, part II: prototype performance evaluation, IEEE Trans. Ultrason. Ferroelectr. Freq. Control 50 (10) (2016) 1351–1362.
[30] Retrieved from: http://www.plansee.com/en/Materials-Tungsten-403.htm.
[31] E.A. Neppiras, Subharmonic and other low-frequency signals from sound-irradiated liquids, J. Sound Vib. 10 (1969) 176–180.
[32] Belorussian State University of Informatics and Radioelectronics, Cavitometer ICA-3HT: Technical Characteristics and Instructions. Minsk, Belarus. (2012).
[33] R.A. Smith, D.R. Bacon, A multiple-frequency hydrophone calibration technique, J. Acoust. Soc. Am. 87 (1990) 2231–2243.
[34] L. Wang, G. Memoli, I. Butterworth, B. Hodnett, Zeqiri, Characterisation of a multi-frequency cavitation vessel, Mater. Sci. Eng. 42 (2012) 012013.
[35] D. Xu, W.K. Jones Jr., J.W. Evans, The use of PIV in the physical modelling of flow in EM or DC casting of aluminium: Part I. Development of the physical model, Metall. Mater. Trans. B 29B (1998) 1281–1288.
[36] L.D. Rozenberg, Cavitation Zone in Powerful Ultrasonic Fields, in: L.D. Rozenberg (Ed.), Nauka, Moscow, 1968, pp. 240–246.
[37] W. Wu, I. Tzanakis, P. Srirangam, S. Terzi, W. Mirihanage, D.G. Eskin, P. Lee, In situ synchrotron radiography of ultrasound cavitation in a molten Al–10Cu alloy, in: J. Mi, D.G. Eskin (Eds.), TMS Supplemental Proceedings, John Wiley & Sons, Hoboken, NJ, USA, 2015, pp. 61–66.
[38] I. Tzanakis, W.W. Xu, G.S.B. Lebon, D.G. Eskin, K. Pericleous, P.D. Lee, In situ synchrotron radiography and spectrum analysis of transient cavitation bubbles in molten aluminium alloy, Phys. Procedia 70 (2015) 841–845.
[39] I. Tzanakis, G.S. Lebon, D.G. Eskin, K. Pericleous, Characterisation of the ultrasonic acoustic spectrum and pressure field in aluminium melt with an advanced cavitometer, J. Mater. Process. Technol. 229 (2016) 582–586.
[40] A. Moussatov, A. Granger, C. Dubus, Cone-like bubble formation in ultrasonic cavitation field, Ultrason. Sonochem. 10 (2003) 191–195.

Biographies

Iakovos Tzanakis, PhD, is a research fellow in Brunel Centre for Advanced Solidification Research at Brunel University London, UK. He also holds an Academic Visitor position in the University of Oxford (UK) since 2013. After graduating with a PhD in Tribology, he worked as a research assistant at Bournemouth University (UK) focusing on the cavitation erosion mechanisms of steel materials and the frictional mechanisms of PTFE composites. Subsequently he moved to Brunel University where he led the research work on the ultrasonic treatment of molten metal alloys and was spearheaded the experimental research work for the EPSRC project UltraMELT. Expanding his academic career, in 2016, Iakovos obtained a lectureship position in Oxford Brookes. Current interests include (b) fundamentals of acoustic cavitation and bubble dynamics in liquid metals and (b) the effect of ultrasound on solidification process. Iakovos is author and co-author of over 30 publications in peer-reviewed journals and conference proceedings.

Mark Hodnett, PhD, was awarded a BSc degree in Physics with Acoustics from the University of Surrey in 1994, and started work at National Physical Laboratory (NPL) in UK in July of that year, commencing NPL's research into measurement techniques for acoustic cavitation. Since then, he has also developed expertise in medical device characterisation, and collaborated on projects as diverse as aerospace NDE to the processing of sewage sludge. Mark is currently leading NPL's work on the development and exploitation of measurement devices and standards in industrial ultrasonics, particularly in high power ultrasound applications such as advanced pharmaceutical and food manufacturing, cleaning, and environmental remediation. He is the lead or co-author of 24 papers in peer-reviewed journals, has written three book chapters, and currently has leadership responsibility for four staff. Mark is the current President of the Ultrasonic Industry Association, and a visiting lecturer at Hammersmith Hospital.

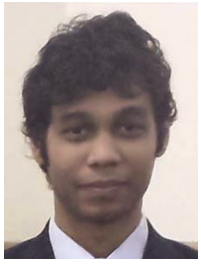

Bruno Lebon, PhD, AMInstP is a post-doctoral research fellow at the University of Greenwich. After graduating with a PhD in Computational Fluid Dynamics, Bruno worked at CD-adapco as an engineer in technical documentation and development support, specialising in turbulence and casting modelling. He is currently spearheading the research work on the modelling of ultrasonic cavitation treatment of liquid aluminium for the EPSRC project UltraMELT.

Nikolai Dezhkunov, PhD, is an Associate Professor and Head of the research Laboratory at the Belarusian State University of Informatics and Radioelectronics (BSUIR). His main research interests are related with phenomena observed in power ultrasound fields, such as acoustic cavitation, ultrasonic capillary effect, sonoluminescence and non-destructive testing. Nikolai is a member of Advisory Board of the European Sonochemical Society, member of Technical Committee for Ultrasonics of the International Commission for Acoustics, member of Russian Acoustical Society and member of Editorial Board of International Electronic Journal *Open Acoustic Journal*. Nikolai has authored 2 books, 47 papers in referred journals, 29 communications and 17 invited lectures 11 of which to peer-reviewed international conferences and 39 patents while he participated in 11 international conferences as a member organizing committees.

Dmitry G. Eskin, PhD, is a Professor in Solidification Research in Brunel Centre for Advanced Solidification Research in Brunel University London. Before that he worked in Institute of Metallurgy, Russian Academy of Sciences and Delft University of Technology in The Netherlands. He also holds a professorship at Tomsk State University (Russia) and he is Editor of Journal of Alloys and Compounds and Series Editor at CRC Press. Prof. Eskin is a well-known specialist in physical metallurgy and solidification processing of light alloys, author and co-author of more than 200 scientific papers, 6 monographs, and a number of patents. His current research focuses on application of ultrasonic cavitation to melt processing. Prof. Eskin is a recipient of Warren Peterson Cast Shop Technology for Aluminum Production Award (2011, 2013) and Aluminum Technology Award (2013) from TMS (USA).